

Dramatic impact of pumping mechanism on photon entanglement in microcavity

Alexander N. Poddubny

Ioffe Physical-Technical Institute RAS, 26 Polytekhnicheskaya, 194021 St.-Petersburg, Russia

(Dated: November 19, 2018)

A theory of entangled photons emission from quantum dot in microcavity under continuous and pulsed incoherent pumping is presented. It is shown that the time-resolved two-photon correlations drastically depend on the pumping mechanism: the continuous pumping quenches the polarization entanglement and strongly suppresses photon correlation times. Analytical theory of the effect is presented.

PACS numbers: 42.50.Ct, 42.50.Pq, 78.66.-m, 78.67.Hc

Semiconductor quantum dots are a promising source of single photons and entangled photon pairs. Polarization-entangled photons generated during the radiative recombination of the quantum dot biexciton are now in a focus of intensive experimental research [1–8].

The state-of-the art approach to increase the rate of photon pair generation is to place the dot in the specially designed cavity, where the frequencies of the two different photon modes are independently tuned to the biexciton and exciton resonances [6]. Both exciton and biexciton radiative recombinations are then increased, allowing to observe bright two-photon emission [6]. Here we study theoretically the quantum emission properties of such microcavity under incoherent pumping. We analyze the polarization density matrix of the photon pair, determined by the second-order correlation function of the photons $g^{(2)}$ [9]. The incoherent pumping itself is an intrinsic feature of the light source. However, to the best of our knowledge, the pumping effect on the biexciton emission has not been theoretically analyzed yet, despite the extensive amount of the studies done [3, 8, 10, 11]. Experimental design of Ref. [6] has not been addressed theoretically as well.

Here we demonstrate that the entanglement is strongly suppressed at incoherent continuous pumping. The qualitative explanation of this effect is presented on Fig. 1. Fig. 1(a) schematically illustrates the cascade of biexciton emission. The radiative recombination of the biexciton leads to the generation of either two horizontally (x) polarized (red arrows), or two vertically (y) polarized (blue arrows) photons in the cavity. When anisotropic exchange splitting of the bright exciton state [12] vanishes, these two channels have the same probability, leading to the completely entangled two-photon state. The situation changes dramatically when the excitons are generated in the quantum dot continuously. One of the possible mechanisms of the entanglement suppression is schematically illustrated on Fig. 1(b). At the first step the biexciton emits x -polarized photon (dotted arrow). After that one x -polarized exciton is remained in the dot. Due to the pumping, another exciton with y polarization can be generated (curved green arrow). This y -polarized exciton can emit photon before the x -polarized one, so

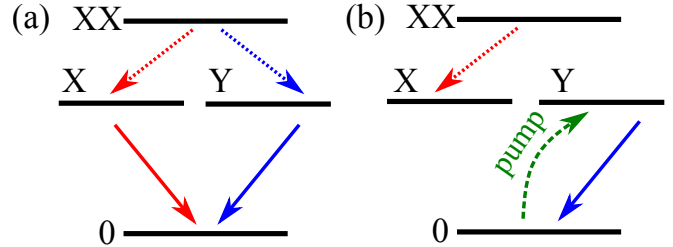


FIG. 1: (Color online) (a) Scheme of the two-photon emission from a quantum dot. Red and blue arrows correspond to x - and y -polarized photon modes, tuned to the exciton (solid arrows) and biexciton (dotted arrows) resonances. The letters 0, X, Y and XX denote ground state, two bright exciton states and biexciton state, respectively. Panel (b) schematically presents the breakdown of the entangled photon emission at continuous pumping.

that a pair of cross-polarized photons is present in the cavity. Such naive analysis hints that the pumping can suppress the generation of entangled photon pairs and raises the demand for more thorough calculation.

To elaborate on this effect we have performed a rigorous simulation based on the master equation for the density matrix of the system [13]. We consider a zero-dimensional microcavity with single quantum dot. The Hamiltonian \mathcal{H} can be written in the following form,

$$\mathcal{H} = \mathcal{H}_{\text{exc}} + \mathcal{H}_{\text{phot}} + \mathcal{H}_{\text{exc-phot}}, \quad (1)$$

where the three terms are the Hamiltonians of the dot, of the cavity photons and of their interaction, respectively. The quantum dot is grown along $z \parallel [001]$ axis from a zinc-blende semiconductor. Only heavy-hole excitons are taken into account. Under the above assumptions the Hamiltonian of the dot reads [12]

$$\mathcal{H}_{\text{exc}} = \sum_{\alpha=x,y,d,d'} \hbar\omega_{X\alpha} n_{X,\alpha} + \hbar\omega_{XX} n_{XX}. \quad (2)$$

The summation in Eq. (2) is performed over x - and y -polarized bright heavy-hole exciton states $|X_{x,y}\rangle$ [12] and over two dark exciton states $|X_{d,d'}\rangle$, with $\hbar\omega_{\text{exc},\alpha}$ being the energies of these states. The singlet biexciton state

with the energy $\hbar\omega_{XX}$ is denoted as $|XX\rangle$. The exciton creation operators a_α^\dagger have the only non-zero matrix elements $\langle X_\alpha|a_\alpha^\dagger|0\rangle = \langle XX|a_\alpha^\dagger|X_\alpha\rangle = 1$. Here $|0\rangle$ is the ground state of the system with no excitations in conduction and valence bands and no photons in the cavity. The operators of exciton and biexciton numbers $n_{X,\alpha}$ and n_{XX} have the only non-zero matrix elements $\langle X_\alpha|n_{X,\alpha}|X_\alpha\rangle = 1$ and $\langle XX|n_{XX}|XX\rangle = 1$, respectively. The anisotropic exchange splitting of the bright exciton doublet is ignored for simplicity. The photon Hamiltonian reads

$$\mathcal{H}_{\text{phot}} = \sum_{\alpha=x,y} \hbar\omega_X c_{1,\alpha}^\dagger c_{1,\alpha} + \sum_{\alpha=x,y} \hbar(\omega_{XX} - \omega_X) c_{2,\alpha}^\dagger c_{2,\alpha}, \quad (3)$$

where $c_{1,\alpha}^\dagger$ and $c_{2,\alpha}^\dagger$ are the creation operators for the two cavity modes with given linear polarization $\alpha = x, y$. We neglect the polarization splitting of the modes and assume, that they are independently tuned to the exciton and biexciton resonances, hereafter we term modes 1 and 2 as exciton and biexciton photon modes, respectively. This corresponds to experimental situation of Ref. [6] Finally, the light-exciton interaction Hamiltonian reads

$$\mathcal{H}_{\text{exc-phot}} = \hbar g \sum_{\substack{\alpha=x,y, \\ \nu=1,2}} (c_{\nu,\alpha}^\dagger a_\alpha + c_{\nu,\alpha} a_\alpha^\dagger), \quad (4)$$

where the interaction constant g is chosen for simplicity real and the same for both modes.

The incoherent pumping leads to the generation of the excitons in the dot [14]. The excitons can decay both radiatively and nonradiatively. The photons, created by exciton recombination, leave the cavity by tunneling through its mirrors, and are detected in experiment. To account for all these processes, one has to solve master equation for the density matrix of the system ρ : [11, 13]

$$\begin{aligned} \frac{d\rho}{dt} \equiv \mathcal{L}\rho &= \frac{i}{\hbar} [\rho, \mathcal{H}] \\ &+ \frac{P_X}{2} \sum_{\alpha=x,y,d,d'} (2a_\alpha^\dagger \rho a_\alpha - a_\alpha a_\alpha^\dagger \rho - \rho a_\alpha a_\alpha^\dagger) \\ &+ \frac{\Gamma_C}{2} \sum_{\substack{\alpha=x,y \\ \nu=1,2}} (2c_{\nu,\alpha} \rho c_{\nu,\alpha}^\dagger - c_{\nu,\alpha}^\dagger c_{\nu,\alpha} \rho - \rho c_{\nu,\alpha}^\dagger c_{\nu,\alpha}) \\ &+ \frac{\Gamma_X}{2} \sum_{\alpha=x,y,d,d'} (2a_\alpha \rho a_\alpha^\dagger - a_\alpha^\dagger a_\alpha \rho - \rho a_\alpha^\dagger a_\alpha). \end{aligned} \quad (5)$$

Here the quantities P_X , Γ_X are the exciton pumping and nonradiative decay rates, and Γ_C is the photon decay rate. For simplicity the polarization and spin dependence of these three processes is disregarded. We note, that the Lindblad terms in (5) describe the generation and decay for both exciton and biexciton states.

In this paper we restrict ourselves to the weak coupling regime for both exciton and biexciton resonances, i.e. $g \ll \Gamma_C$. We also note, that in typical experiments

$\Gamma_X \ll \Gamma_C$ [15–17]. Our goal is to determine the two-photon density matrix

$$\begin{aligned} \rho_{\alpha,\beta;\alpha'\beta'}^{(2)}(t, \tau) &= \mathcal{N} \left\langle \chi_{\alpha'\beta'}^\dagger \chi_{\alpha\beta} \right\rangle, \\ \chi_{\alpha\beta}(t, \tau) &= c_{1,\alpha}(t + \tau) c_{2,\beta}(t), \end{aligned} \quad (6)$$

describing the correlations between the biexciton photon emitted at the time t and the exciton photon emitted at the time $t + \tau$. The angular brackets denote both statistical and quantum mechanical averaging, the constant \mathcal{N} in Eq. (6) is determined from the normalization condition $\text{Tr} \rho^{(2)} = 1$.

Depending on the experimental conditions, two qualitatively different situations can be realized: pulsed pumping and continuous pumping. The procedure to determine $\rho^{(2)}$ is different in these two cases.

(i) *Pulsed pumping.* In this regime we assume that short single pumping pulse creates the population of excitons and biexcitons in the quantum dot. After the pump switches off, the excitons start to recombine radiatively. Assuming that the pulse duration (5 ps in experiment of Ref. 6) is longer than the typical energy relaxation times of the carriers (being on subpicosecond scale [18]), but still shorter than the excitonic radiative lifetime $1/\Gamma_{\text{rad}} = \Gamma_C/(4g^2)$, being on the order of 100 ps [6], we can separate the calculation into two steps. First, we find the density matrix ρ_0 , generated by the pump pulse, from the equation $\mathcal{L}_0 \rho_0 = 0$, where the Liouvillian \mathcal{L}_0 differs from the Liouvillian \mathcal{L} in Eq. (5) by neglecting the coupling term, $g = 0$. Second, we consider the spontaneous decay after the pump is switched off. This process is described by another Liouvillian, $\mathcal{L}_{\text{decay}}$, where exciton-photon coupling is retained but the pumping P_X is set to zero. Thus, we obtain a spontaneous emission problem, with initial conditions determined by the pump. The two-time correlator $\rho^{(2)}(t, \tau)$ then formally reads [13]

$$\begin{aligned} \rho_{\alpha,\beta;\alpha'\beta'}^{(2)}(t, \tau) &= \\ &\mathcal{N} \text{Tr} \left[c_{2\beta'}^\dagger c_{2\beta} e^{\mathcal{L}_{\text{decay}} \tau} \left(c_{1\alpha} \exp^{\mathcal{L}_{\text{decay}} t} \rho_0 c_{1\alpha'}^\dagger \right) \right]. \end{aligned} \quad (7)$$

(ii) *Continuous pumping.* In this case it is assumed, that the excitons are continuously generated in the quantum dot. The balance between the exciton generation and decay leads to the formation of the stationary density matrix ρ , found from the stationary solution of Eq. (5). This density matrix allows us to determine stationary particle numbers. The two-photon density matrix (6) depends only on the delay τ and is given, similarly to Eq. (7), by

$$\rho_{\alpha,\beta;\alpha'\beta'}^{(2)}(\tau) = \mathcal{N} \text{Tr} \left[c_{2\beta'}^\dagger c_{2\beta} e^{\mathcal{L} \tau} \left(c_{1\alpha} \rho c_{1\alpha'}^\dagger \right) \right]. \quad (8)$$

The density matrix equations were solved numerically expanding the density matrix over the complete basis of

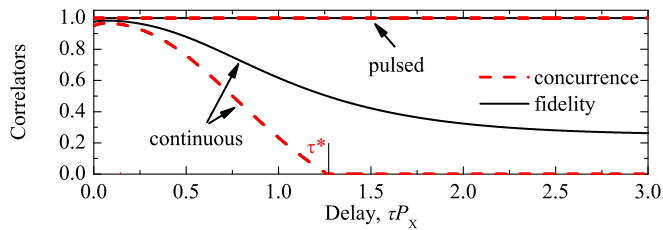


FIG. 2: (Color online) Time dependence of concurrence (dashed lines) and fidelity (solid lines) at continuous and pulsed pumping. Calculation was performed at the following set of parameters: $\hbar g = 30 \mu\text{eV}$, $\hbar\Gamma_X = 15 \mu\text{eV}$, $\hbar\Gamma_C = 300 \mu\text{eV}$, $\hbar\omega_{XX} - 2\hbar\omega_X = -5 \text{ meV}$, $P_X = 0.1\Gamma_C$.

the quantum dot and the cavity states. The resulting matrices of Liouvillians are sparse, which makes the calculation of the matrix exponentials feasible. Some analytical results in stationary regime will be presented below.

The obtained two-photon polarization density matrix has the following general structure:

$$\rho^{(2)}(\tau) = \frac{1}{2(N_{\parallel} + N_{\perp})} \begin{pmatrix} N_{\parallel} & 0 & 0 & N_{\odot} \\ 0 & N_{\perp} & 0 & 0 \\ 0 & 0 & N_{\perp} & 0 \\ N_{\odot} & 0 & 0 & N_{\parallel} \end{pmatrix}, \quad (9)$$

where the order of matrix elements is x_1x_2 , x_1y_2 , y_1x_2 , y_1y_2 . Here the quantities N_{\parallel} and N_{\perp} determine the probability of the detection of excitonic and biexcitonic photons with matching and different linear polarizations, respectively. The matrix element N_{\odot} describes the correlations of clockwise and counter-clockwise circularly polarized photons. The structure of the density matrix (9) is similar to that obtained in Ref. 2. However, in our case the suppression of the entanglement is solely related to the pumping and the quantity N_{\odot} is real. The concurrence of the state (9), quantifying the entanglement [9], reads

$$C = \max \left\{ \frac{N_{\odot} - N_{\perp}}{N_{\parallel} + N_{\perp}}, 0 \right\}. \quad (10)$$

The results of calculation are presented on Fig. 2. For pulsed pumping one has $N_{\odot} = N_{\parallel} = 1$ and $N_{\perp} = 0$, which corresponds to the completely entangled Bell state,[9] where fidelity and concurrence are both equal to unity. For continuous pumping both concurrence and fidelity are smaller than unity, and are suppressed at large delays τ . After a certain delay τ^* the concurrence is zero, i.e. the state is not entangled. Entanglement suppression is directly related to the incoherent nature of the pumping. Indeed, excitons are constantly generated in the dot, and then eventually emit photons. As soon as the delay becomes larger, than the dot repopulation time, the temporal coherence of the photons is lost. At very large delay one has $N_{\parallel} = N_{\perp} = 1/4$ and $N_{\odot} = 0$, which corresponds to completely independent photons.

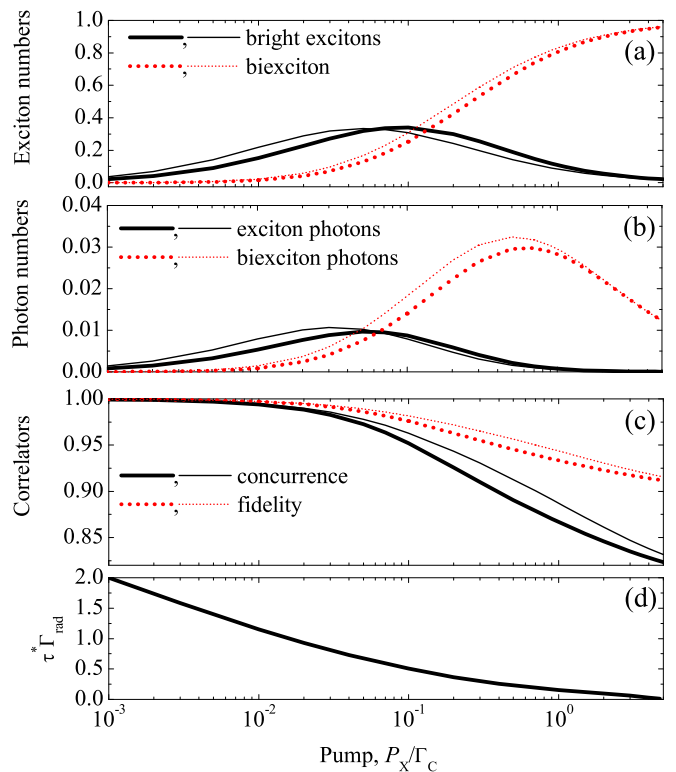


FIG. 3: (Color online) Stationary particle numbers and correlators as function of pumping. (a) The total numbers of bright excitons (solid curves) and biexciton (dotted curves) photons as functions of pumping. (b) The numbers of exciton (solid curves) and biexciton (dashed curves) photons as functions of pumping. (c) Concurrence (solid curves) and fidelity (dotted curves) of the two-photon pair at zero delay, $\tau = 0$. (d) Concurrence lifetime τ^* , divided by exciton radiative lifetime $1/\Gamma_{\text{rad}}$. Thick curves are results of numerical calculation, thin curves present the analytical results of Supplemental Materials. Calculated at the same parameters as Fig. 2.

Fig. 3 presents more detailed analysis of stationary correlators. Interestingly, even the stationary entanglement, calculated at $\tau = 0$, is suppressed by the pumping. First two panels present the calculated bright exciton, biexciton and photon occupation numbers as functions of pumping. Thick lines correspond to the results of the numerical calculation. Thin lines present the analytical results in weak coupling regime, obtained in Supplemental Materials. Here we briefly summarize them. Neglecting the exciton-photon coupling one can get stationary exciton population numbers

$$N_{X,\alpha} = \frac{P_X}{\Gamma_X + 4P_X + P_X^2/\Gamma_X}, \quad N_{XX} = \frac{P}{\Gamma_X} N_{X,x}, \quad (11)$$

where $\alpha = x, y, d, d'$. Eq. (11) indicates that at small pumpings N_X increases linearly with pumping, and N_{XX} increases quadratically. At high pumping the dot is in biexciton state, i.e. $N_{XX} \rightarrow 1$ and $N_X \rightarrow 0$. The photon

numbers $N_{C,\alpha}^{(1,2)}$ in the weak coupling regime are given by

$$\Gamma_C N_{C,\alpha}^{(1)} = 2\pi g^2 N_{X,\alpha} \varrho_1, \quad \Gamma_C N_{C,\alpha}^{(2)} = 2\pi g^2 N_{XX} \varrho_2 \quad (12)$$

where

$$\varrho_1 = \frac{2}{\pi(\Gamma_C + \Gamma_X + 5P_X)}, \quad \varrho_2 = \frac{2}{\pi(\Gamma_C + 5\Gamma_X + P_X)},$$

and $\alpha = x, y$. The right hand sides in Eqs. (12) are the rates of photon generation due to exciton recombination. They are presented in the form similar to the Fermi Golden rule and have simple physical meaning: the rate is proportional to the population of the correspondent state of the dot, to the square of the interaction constant g and to the effective density of states ϱ . The latter is quenched at high pumping due to the fermionic nature of the electrons, which typically leads to the pumping-induced linewidth broadening [19, 20]. Thus, at small pumping the exciton and biexciton photon numbers are proportional to the population of the corresponding quantum dot states, and at high pumpings they are suppressed by the pumping-induced dephasing. This explains the behavior of the curves on Fig. 3b.

At the vanishing pumping one has $N_{\circ}(\tau = 0) = N_{\parallel}(\tau = 0) = 1$ and $N_{\perp}(\tau = 0) = 0$ in Eq. (9), which corresponds to the completely entangled Bell state with concurrence $C = 1$, see Eq. (10). The pumping leads to the growth of N_{\perp} and to the suppression of N_{\circ} . This quenches the entanglement, in agreement with Fig. 3(c). Fig. 3(d) demonstrates that the concurrence lifetime τ^* , i.e. the time, during which the state remains entangled, decreases with pumping, because the dot is faster repopulated. We note, that the high sensitivity of two-photon correlations to the pumping is a rather general effect, known, for instance, in superradiant emission of the cavities with several resonant quantum dots [21] or for single-dot lasers [22]. The main result of Fig. 3 is that the entanglement degree is substantially quenched when the pumping is large enough to make the numbers of exciton and biexciton photons comparable.

To summarize, we have put forward a general theory of the entangled photon generation from the zero-dimensional microcavity with embedded quantum dot under incoherent pumping in the weak coupling regime. We have demonstrated that the time-dependent polarization density matrix of the entangled photon pair is very sensitive to the mechanism of pumping, i.e. pulsed one or continuous one. Analytical theory of this effect has been presented. Important goal of the future studies is to analyze the strong coupling regime, up to now realized only for the exciton resonance [15, 16].

The author acknowledges encouraging discussions with M.M. Glazov, E.L. Ivchenko and P. Senellart. This work has been supported by RFBR, ‘‘Dynasty’’ Foundation-ICFPM, and the projects ‘‘POLAPHEN’’ and ‘‘Spin-Optronics’’.

- [1] N. Akopian, N. H. Lindner, E. Poem, Y. Berlatzky, J. Avron, D. Gershoni, B. D. Gerardot, and P. M. Petroff, Phys. Rev. Lett. **96**, 130501 (2006).
- [2] A. J. Hudson, R. M. Stevenson, A. J. Bennett, R. J. Young, C. A. Nicoll, P. Atkinson, K. Cooper, D. A. Ritchie, and A. J. Shields, Phys. Rev. Lett. **99**, 266802 (2007).
- [3] R. M. Stevenson, A. J. Hudson, A. J. Bennett, R. J. Young, C. A. Nicoll, D. A. Ritchie, and A. J. Shields, Phys. Rev. Lett. **101**, 170501 (2008).
- [4] A. Muller, W. Fang, J. Lawall, and G. S. Solomon, Phys. Rev. Lett. **103**, 217402 (2009).
- [5] A. J. Bennett, M. A. Pooley, R. M. Stevenson, M. B. Ward, R. B. Patel, A. B. de La Giroday, N. Sköld, I. Farrer, C. A. Nicoll, D. A. Ritchie, et al., Nature Physics **6**, 947 (2010).
- [6] A. Dousse, J. Suffczynski, A. Beveratos, O. Krebs, A. Lemaitre, I. Sagnes, J. Bloch, P. Voisin, and P. Senellart, Nature **466**, 217 (2010).
- [7] M. Kaniber, M. F. Huck, K. Müller, E. C. Clark, F. Troiani, M. Bichler, H. J. Krenner, and J. J. Finley, Nanotechnology **22**, 325202 (2011).
- [8] Y. Ota, S. Iwamoto, N. Kumagai, and Y. Arakawa, ArXiv e-prints (2011), 1107.0372.
- [9] D. F. V. James, P. G. Kwiat, W. J. Munro, and A. G. White, Phys. Rev. A **64**, 052312 (2001).
- [10] R. Johne, N. A. Gippius, G. Pavlovic, D. D. Solnyshkov, I. A. Shelykh, and G. Malpuech, Phys. Rev. Lett. **100**, 240404 (2008).
- [11] E. del Valle, S. Zippilli, F. P. Laussy, A. Gonzalez-Tudela, G. Morigi, and C. Tejedor, Phys. Rev. B **81**, 035302 (2010).
- [12] E. L. Ivchenko, *Optical spectroscopy of semiconductor nanostructures* (Alpha Science International, Harrow, UK, 2005).
- [13] H. Carmichael, *An Open Systems Approach to Quantum Optics* (Springer, New York, 1993).
- [14] N. S. Averkiev, M. M. Glazov, and A. N. Poddubny, JETP **108**, 836 (2009).
- [15] T. Yoshie, A. Scherer, J. Hendrickson, G. Khitrova, H. M. Gibbs, G. Rupper, C. Ell, O. B. Shchekin, and D. G. Deppe, Nature **432**, 200 (2004).
- [16] J. P. Reithmaier, G. Sek, A. Löffler, C. Hofmann, S. Kuhn, S. Reitzenstein, L. V. Keldysh, V. D. Kulakovskii, T. L. Reinecke, and A. Forchel, Nature **432**, 197 (2004).
- [17] E. Peter, P. Senellart, D. Martrou, A. Lemaitre, J. Hours, J. M. Gérard, and J. Bloch, Phys. Rev. Lett. **95**, 067401 (2005).
- [18] C. Delerue and M. Lanoo, *Nanostructures. Theory and Modelling* (Springer Verlag, Berlin, Heidelberg, 2004).
- [19] E. del Valle, F. P. Laussy, and C. Tejedor, Phys. Rev. B **79**, 235326 (2009).
- [20] A. N. Poddubny, M. M. Glazov, and N. S. Averkiev, Phys. Rev. B **82**, 205330 (2010).
- [21] V. V. Temnov and U. Woggon, Opt. Express **17**, 5774 (2009).
- [22] J. Wiersig, C. Gies, F. Jahnke, M. Aßmann, T. Berstermann, M. Bayer, C. Kistner, S. Reitzenstein, C. Schneider, S. Höfling, et al., Nature **460**, 245 (2009).

Supplemental material

S1. Stationary exciton and photon numbers

Now we obtain the stationary occupation numbers of the quantum dot states and the stationary photon numbers, Eq. (12) and Eq. (11). We consider the weak coupling regime, and assume that the additional condition

$$\Gamma_C \gg \Gamma_{\text{rad}}, \text{ i.e. } \Gamma_C \Gamma_X \gg g^2, \quad (\text{S1})$$

holds. Our goal is to expand the density matrix in powers of the coupling constant g ,

$$\rho = \rho_0 + \rho_1 + \dots, \quad \rho_j \propto g^j. \quad (\text{S2})$$

The lowest order contribution to exciton number is determined by ρ_0 and does not depend on g , while the photon numbers are proportional to g^2 . To perform the expansion we express the total Liouvillian \mathcal{L} of the system (5) as $\mathcal{L}_0 + \mathcal{L}_1$, where \mathcal{L}_0 is the Liouvillian neglecting exciton-photon interaction, and

$$\mathcal{L}_1 \rho \equiv \frac{i}{\hbar} [\rho, \mathcal{H}_{\text{exc-phot}}]. \quad (\text{S3})$$

The zero-order contribution to the stationary density matrix is found from the equation

$$\mathcal{L}_0 \rho_0 = 0. \quad (\text{S4})$$

Each following term of the expansion (S2) is determined by the recurrence relation

$$-\mathcal{L}_0 \rho_j = \frac{i}{\hbar} [\rho_{j-1}, \mathcal{H}_{\text{exc-phot}}]. \quad (\text{S5})$$

Let us first solve Eq. (S4). Obviously, the matrix ρ_0 is diagonal, with the only non-zero matrix elements

$$\begin{aligned} \langle X, \alpha | \rho_0 | X, \alpha \rangle &= N_{X,\alpha} \equiv N_X, & (\text{S6}) \\ \langle XX | \rho_0 | XX \rangle &= N_{XX}, \\ \langle 0 | \rho_0 | 0 \rangle &= 1 - N_{XX} - 4N_X, \end{aligned}$$

where we took into account the normalization condition $\text{Tr} \rho_0 = 1$. Substituting the density matrix in the form (S6) into Eq. (S4) we obtain the following system of linear equations:

$$\begin{aligned} -(\Gamma_X + P_X)N_X + \Gamma_X N_{XX} + P_X(1 - N_{XX} - 4N_X) &= 0, \\ -\Gamma_X N_{XX} + P_{XX}N_X &= 0. \end{aligned} \quad (\text{S7})$$

Solution of this system yields Eq. (11).

Now we proceed to the calculation of the stationary photon numbers. We consider the case of the x -polarized biexciton photons as an example. Calculating the commutator Eq. (S5) for the term $N_{XX}|XX\rangle\langle XX|$, entering ρ_0 , we get

$$\frac{i}{\hbar} [\rho_0, \mathcal{H}_{\text{exc-phot}}] = \frac{igN_{XX}}{\hbar} b^\dagger |0\rangle\langle 0| ac_{2,x} + h.c. \quad (\text{S8})$$

Assuming, that the binding energy of the biexciton $\omega_{XX} - 2\omega_X$ is much larger than P_X , Γ_C , Γ_X and g , we write down Eq. (S5) to find biexciton-related term in ρ_1 :

$$\frac{1}{2}(\Gamma_C + 5\Gamma_X + P_X)\rho_1 = \frac{igN_{XX}}{\hbar} b^\dagger |0\rangle\langle 0| ac_{2,x} + h.c. \quad (\text{S9})$$

Finding ρ_1 and calculating the commutator (S5) again, we obtain the generation rate of the biexciton photons, standing in the r.h.s. of Eq. (12). We see, that Eq. (S9) yields the density of states ϱ_2 . The value of ϱ_2 is inversely proportional to the decay rate in l.h.s. of Eq. (S9). Eq. (12) is in fact the particular case of Eq. (S5) to find the matrix ρ_2 , averaged over the states of the dot. Analogous procedure yields the generation rate of the exciton photons. The consideration differs only in the decay rate of the intermediate state of type $a^\dagger |0\rangle\langle 0| c_1$, equal to π/ϱ_1 .

S2. Stationary two-photon density matrix

In this Section we present the explicit results for the two-photon stationary density matrix (9). The calculation procedure is generally the same as that presented above to obtain the stationary photon numbers. However, it requires expansion of the stationary density matrix up to the fourth term in the series over g (S2), proportional to g^4 . The calculation is therefore much more tedious, but still feasible. Thus, we will only present the results:

$$N_{\parallel} \equiv \langle c_{2,x}^\dagger c_{1,x}^\dagger c_{1,x} c_{2,x} \rangle = \frac{\pi g^2}{\Gamma_C} [AN_{1,XX} + A'N_{2,\parallel} + BN_{XX}], \quad (\text{S10})$$

$$N_{\circlearrowleft} \equiv \langle c_{2,x}^\dagger c_{1,x}^\dagger c_{1,y} c_{2,y} \rangle = \frac{\pi g^2}{\Gamma_C} [A'N_{2,\circlearrowleft} + BN_{XX}], \quad (\text{S11})$$

$$N_{\perp} \equiv \langle c_{2,x}^\dagger c_{1,y}^\dagger c_{1,y} c_{2,x} \rangle = \frac{\pi g^2}{\Gamma_C} [AN_{1,XX} + A'N_{2,\perp}] \quad (\text{S12})$$

where

$$A = \frac{2}{\pi(3\Gamma_C + 5\Gamma_X + P_X)}, \quad A' = \frac{2}{\pi(3\Gamma_C + \Gamma_X + 5P_X)}, \quad (\text{S13})$$

$$G = \frac{\pi g^2 AA'}{\Gamma_C + 2\Gamma_X + 2P_X}, \quad N_{2\circlearrowleft} = \frac{\Gamma_C N_{C,x}^{(2)}}{\Gamma_C + \Gamma_X + P_X}.$$

The correlator $N_{1,XX}$ is readily found from the linear system

$$\begin{aligned} -(\Gamma_C + 4P_X)N_{1G} + 4\Gamma_X N_{1G} &= -2\pi g^2 N_{X,x} \varrho_1, & (\text{S14}) \\ -(\Gamma_C + \Gamma_X + P_X)N_{1X} + N_{1G}P_X + N_{1XX}\Gamma_X &= 0, \\ -(\Gamma_C + 4\Gamma_X)N_{1XX} + 4N_{1X}P_X &= 0. \end{aligned}$$

Here the quantities $N_{1,G}$, $N_{1,X}$ and $N_{1,XX}$ determine the probabilities to find one exciton photon and the dot in ground, excitonic and biexciton states, respectively. The correlators $N_{2,\parallel}$ and $N_{2,\perp}$ are found from

$$\begin{aligned}
-(\Gamma_C + 4P_X)N_{2,G} + \Gamma_X(N_{2,\parallel} + N_{2,\perp} + 2N_{2,\text{dark}}) &= 0, \\
-(\Gamma_C + \Gamma_X + P_X)N_{2,\parallel} + N_{2,G}P_X + N_{2,XX}\Gamma_X &= \\
&\quad - 2\pi g^2 N_{XX}\varrho_2, \\
-(\Gamma_C + \Gamma_X + P_X)N_{2,\perp} + N_{2,G}P_X + N_{2,XX}\Gamma_X &= 0, \\
-(\Gamma_C + \Gamma_X + P_X)N_{2,d} + N_{2,G}P_X + N_{2,XX}\Gamma_X &= 0 \\
-(\Gamma_C + 4\Gamma_X)N_{2,XX} + (N_{2,\parallel} + N_{2,\perp} + 2N_{2,d})P_X &= 0.
\end{aligned} \tag{S15}$$

Here $N_{2,G}$, $N_{2,\parallel}$, $N_{2,\perp}$, $N_{2,d}$, and $N_{2,XX}$ are the probabilities to find one x -polarized biexciton photon and the dot in the ground state, x exciton state, y exciton state, dark exciton state and biexciton state, respectively.

Let us comment on the calculation details. The equations for ρ_1 and ρ_3 are similar to Eq. (S9) and yield

the denominators given by the pumping-dependent decay rates, see Eq. (S13). Final equation to find the two-photon density matrix $\rho^{(2)}$, corresponding to $j = 4$, is trivial, since we are interested only in the value of $\rho^{(2)}$ traced over the states of the dot. This equation yields the prefactor $\propto 1/\Gamma_C$ in Eqs. (S10)–(S12). However, equations (S14) and (S15) to find the components of the density matrix ρ_2 become nontrivial. These equations explicitly depend on the pumping. For instance, the quantity $N_{2,\perp}$ describes the probability, that the y -polarized exciton is generated in the quantum dot, after the x -polarized biexciton is emitted. Such process contributes to the correlator (S12) and destroys the entanglement. It is illustrated on Fig. 1b. Another similar pumping-induced process is the the absorption of the biexciton in the dot after the emission of the exciton photon. It is described by the correlator $N_{1,XX}$ and also contributes to Eq. (S12). At the vanishing pumping both these processes are quenched, which leads to the totally entangled state with $N_{\parallel} = N_{\odot}$, $N_{\perp} = 0$.